ALLPLAN
A NEMETSCHEK COMPANY

DESIGN TO BUILD
COMPETENCE IN PRECAST

THE BEST SOLUTIONS FOR YOUR PRECAST PROJECTS

- **Automated workflows** to accelerate design and detailing processes
- **Automated creation** of shop drawings and production data
- **Quality assured data** for ERP and MES

FIND OUT MORE NOW:
allplan-precast.com

Received: 18 August 2021 | Revised: 1 November 2021 | Accepted: 24 November 2021

DOI: 10.1002/suco.202100561

ARTICLE

fib CEB-FIP WILEY

Longitudinal shear in the tension flanges of composite concrete beams made continuous

Ulla Kytölä | **Joonas Tulonen** | **Anssi Laaksonen**

Unit of Concrete and Bridge Structures, Tampere University, Tampere, Finland

Correspondence
Ulla Kytölä, Unit of Concrete and Bridge Structures, Tampere University, Tampere, Finland.
Email: ulla.kytola@tuni.fi

Funding information
Finnish Concrete Industry

Abstract

In continuous concrete T-beams, tension flange plays a remarkable role for the hogging moment capacity at the support area. When precast beams are connected as a continuous structure, longitudinal reinforcement is spread in the flange overhangs at the negative moment area of the continuity connection, which causes longitudinal shear in the tension flange's web-flange junction. The level of reinforcement spreading influences the magnitude of in-plane forces at the junction, which can cause the flanges to crack and eventually separate from the web. This separation must be prevented by providing transversal reinforcement in the flanges. Longitudinal shear between web and flange and the required transversal reinforcement are experimentally and computationally studied in cantilever composite T-beams with the flange in tension. A comparison of the experimental and computational results revealed that longitudinal shear distribution in accordance with conventional beam theory does not always yield safe side results. Analyses made with a particularly drawn truss model and the modified compression field theory are in better agreement with the experimental results.

KEYWORDS

continuity connection, longitudinal shear, MCFT, T-beams, tension flange, transverse reinforcement

1 | INTRODUCTION

Underground parking has gained in popularity, with space in high-density and valuable land areas being freed up for more active uses. Deck structures at ground level are usually heavily loaded, laborious to design, and expensive to construct. The capacity of normal simple-span prestressed concrete girders is often insufficient for carrying these heavy deck loads combined with the required span lengths. In order for precast prestressed beams in these deck structures to be utilized, the application of the structure needs to be improved.

A common way in bridge construction for increasing the capacity of single span precast prestressed beams is to connect them to a continuous structure. Continuity is achieved with an in situ cast deck slab and diaphragm over intermediate support. In this method, the girders

Discussion on this paper must be submitted within two months of the print publication. The discussion will then be published in print, along with the authors' closure, if any, approximately nine months after the print publication.

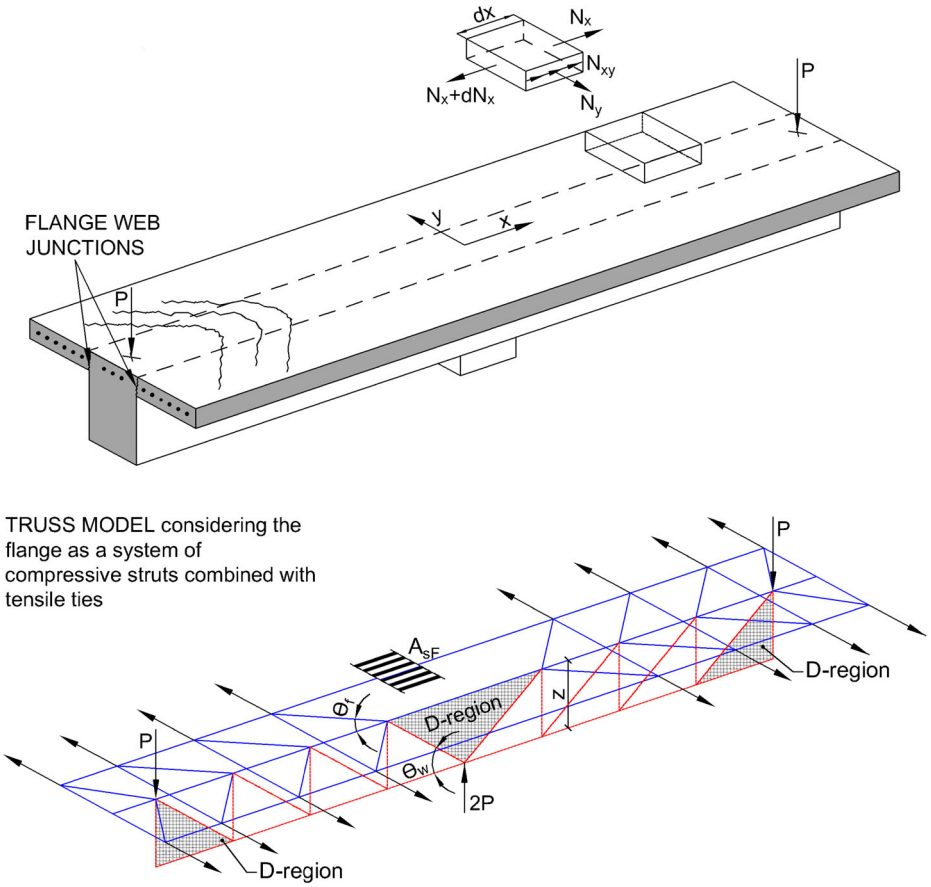

FIGURE 1 Membrane forces at the flange-web junctions in the tension flange of the T-beam (modified from Razaqpur and Ghali[10])

behave as simple spans for dead loads before the continuity is achieved. After that, the composite section of the prestressed beam and cast-in-place deck slab bear the superimposed dead and live loads as a continuous girder. Throughout this article, the term *composite beam* will refer to a hybrid structure which is a combination of a prestressed precast concrete girders and an in situ cast concrete slab.

In a continuous girder, mid-span flexural moments and maximum deflections are reduced and moment redistribution is possible. This paper is part of a dissertation which purpose is to explore the potentials single span, prestressed concrete beams made continuous in heavily loaded parking deck structures. A recently published paper[1] is a part of the same dissertation and studies negative moment capacity of the structure.

A general procedure to create continuity between precast beams is to embed reinforcing bars across supporting piers in a situ-cast deck slab to provide the negative moment continuity.[2–4] When the amount of longitudinal reinforcement providing negative moment capacity is high, the tensile reinforcement is commonly distributed in the flange overhangs of the composite T-section. It has been suggested that reinforcement of the tension flange should be spread to a wider breadth than the web to control the crack widths of the flange. If the reinforcement is concentrated over the web, the amount of cracks can remain small but crack widths increase considerably.[5,6]

When the flange of a T-beam participates with the web in resisting flexural forces, the integrity of the junctions of the flanges with the web must be preserved. This means that adequate transversal reinforcement must be provided regardless of whether the flange is in tension or in compression. If the beams have no transverse reinforcement in their flanges, the separation of the flanges from the web will cause a premature failure of the beam once cracking occurs at the web-flange junction. Clearly, it cannot be accepted that a flange falls off. Minimum nominal transverse reinforcement should be sufficient to avoid this, but it will not necessarily ensure that the flange continues to work properly as part of the cross section after cracking.[7]

Eurocodes suggest procedures for considering longitudinal shear between web and flanges of T-section and provide guidance in determining transverse reinforcement to the flanges.[8,9] European guidance allows longitudinal shear in the flanges to be checked using a truss model (TM; see Figure 1) or from elastic cross-sectional analysis using beam theory.[11] Previous research has established that these methods lead in general to a safe design of the transverse

reinforcement of compression flanges, but they may also yield unsafe results for tension flanges, even if there is no transverse bending.[12]

The function of continuity connection between precast prestressed beams made continuous has been extensively studied. However, less attention has been paid to the decks' transversal reinforcement. According to the AASHTO design specifications, section "Bridges Composed of Simple Span Precast Girders Made Continuous," all longitudinal reinforcement of the deck slab may be used for the negative moment connection. Required transversal reinforcement has not received any attention at the specifications.[13] In precast prestressed bridges, the beams are placed close together and the flange width is limited. In the bridges, the self-weight of the girders is the major part of the loading and the negative moment over supports is often minor; as a result, the amount of longitudinal reinforcement at the top plate is insignificant. The situation is different in parking deck structures, where the beam-to-beam distance might be several meters and the load after continuity connection pays a considerable role. When the amount of tensile top reinforcement increases, the need to spread it wider to the overhangs becomes necessary. Subsequently, the need for transversal reinforcement becomes more critical.

The objective of this research is to provide experimental results and study the longitudinal shear between the flange and the web at intermediate support in composite precast beams made continuous. Hogging moment area of the continuous structure is isolated as a cantilever beam and studied. This paper provides an overview from simple to more precise available methods for analyzing longitudinal shear at the web-flange junction of the tension flange. Theoretical results are compared to experimental values and discussed. It is hoped that this research will contribute to a deeper understanding of the required transverse reinforcement of the studied structure.

2 | DESIGN OF TRANSVERSE REINFORCEMENT IN TENSION FLANGES OF T-BEAMS

When the loads are applied over the web of the T-shaped cross section as shown in Figure 1, the flanges near their junctions with the web are subjected to membrane forces N_x, N_y, and N_{xy}, where x and y are the horizontal axes parallel and perpendicular to the beam axis. These forces can cause cracking in the flanges along the web-flange junction. If sufficient reinforcement is not provided, the cracks will lead to separation of the flanges from the web. The definition of tensile forces N_x and $N_x + dNx$ is quite straightforward, according to the conventional beam theory (CBT), while the assessment of N_{xy} and N_y is rather controversial. Note that in this paper, N_x, N_y, and N_{xy} are assumed to be force per unit length, and σ_x, σ_y, and τ_{xy} are assumed to be stresses. The next section concerns the generally used methods to evaluate longitudinal shear and transversal stresses and forces in design. The central thesis of this paper is to study longitudinal shear in the tension flanges. Although transverse bending moment and vertical shear has also influence on transverse reinforcement of the studied structure they are not included in this study. For the sake of clarity, this paper concentrates on only one isolated component of the phenomenon.

2.1 | Web-flange longitudinal shear stress τ_{xy} distribution

Longitudinal shear stress τ_{xy}, at the junction between one side of a flange and the web of the tension flange, can be determined according to elastic cross-sectional analysis using the CBT. Shear stress at the cracked stage can be approximated by Equation (1) or (2). In the structure studied in this paper, both approaches yield the same results.

$$\tau_{xy} = \frac{\Delta N_{fx}}{\Delta x h_f} \tag{1}$$

where ΔN_{fx} is the change in the normal force in one side of the flange over the length Δx and Δx is the length under consideration.

The maximum value that may be assumed for Δx is half the distance between the cross section where the moment is 0 and the section where the moment is maximum. Where point loads are applied, the length Δx should not exceed the distance between point loads.[9–11]

$$\tau_{xy} = \frac{V}{z h_f} \frac{A_{sF}}{A_s} \tag{2}$$

where V is the shear force of the cross section, z is the inner lever arm, corresponding to the bending in the cross section, A_{sF} is part of A_s, placed in one flange overhang, A_s is the total amount of the flexural reinforcement area, and h_f is the thickness of the flange at the junction.

2.2 | Transversal stress σ_y

Two most common methods available to define the variation of transversal stress σ_y are based on the τ_{xy}

distribution and truss analogy. One option is to draw out detailed TM for the structure (see Figure 1). This strut and tie model covers the crushing resistance of the concrete struts and the tensile strength of the transverse reinforcement. Another less labor-consuming practical design approach is to avoid the need to draw TMs and determine longitudinal shear from elastic cross-sectional analysis using beam theory. According to CBT,[9,11,14] σ_y can be determined with Equation (3)

$$\sigma_y = \tau_{xy} \tan \theta_f \tag{3}$$

where θ_f is the angle of transversal compressive struts in the flange (Figure 1).

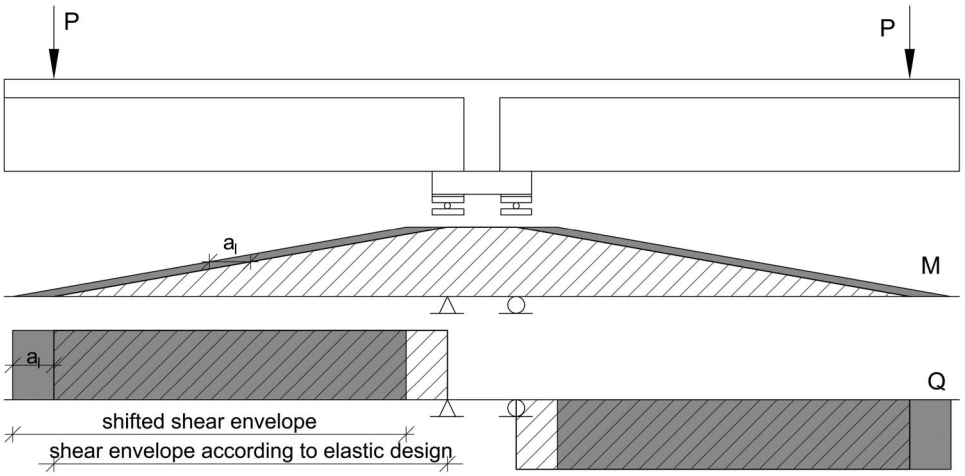

FIGURE 2 Shear envelope of cantilever beam according to elastic design and considering the "shift rule"

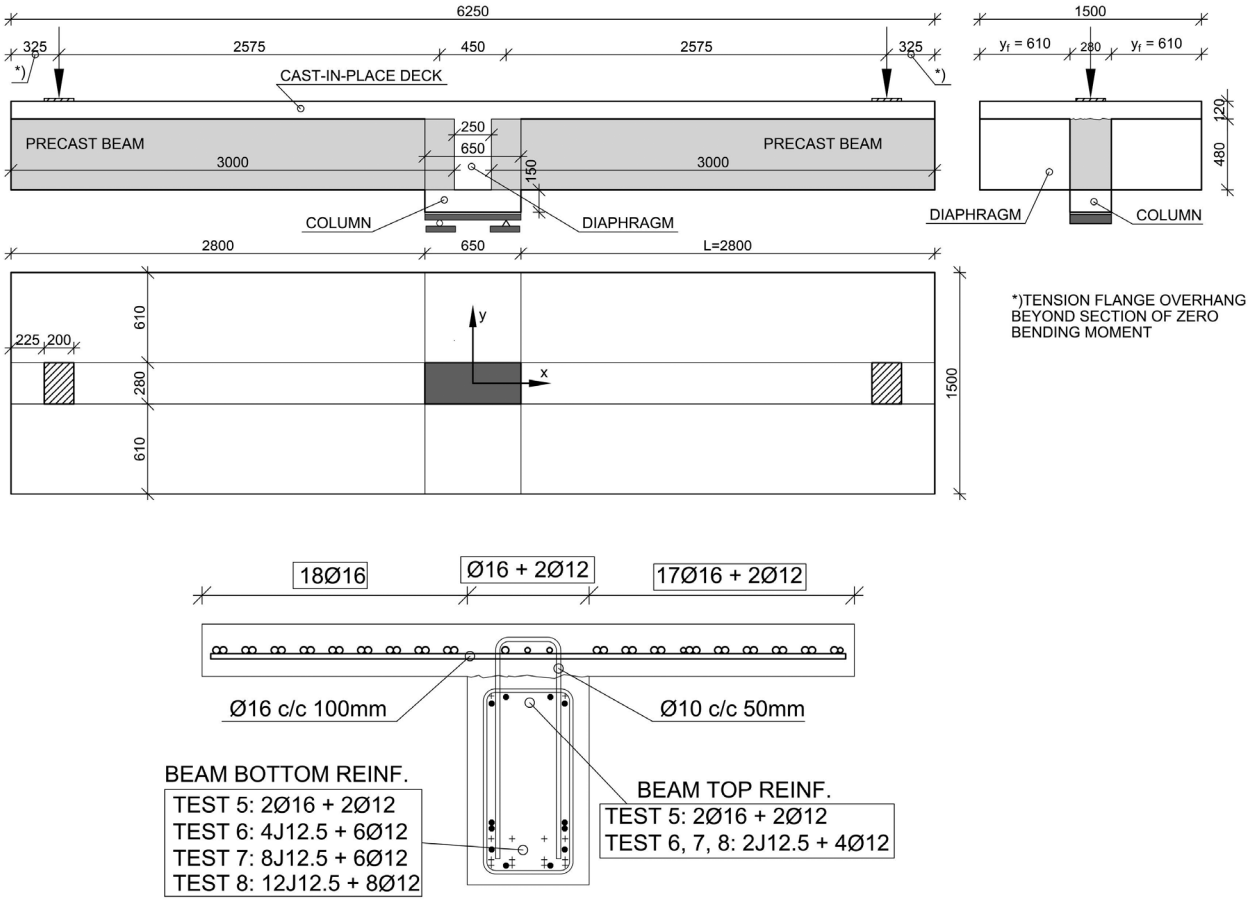

FIGURE 3 General data of the test beams

Various values for the angle of the tension flange transversal compression strut of the truss can be found in the literature. According to References 9, 15, and 16, the recommended values for the angle spread are $38.6^\circ \leq \theta_f \leq 45^\circ$, $26.7^\circ \leq \theta_f \leq 35^\circ$, and $35^\circ \leq \theta_f \leq 50^\circ$, respectively. On a result of these recommendations, $\tan\theta_f$ varies between 0.5 and 1.2.

The method of calculating flange shear stress from the vertical shear force envelope of the beam gives only approximate information on where to place transverse reinforcement along the beam. It is advised to "shift" the shear force envelope to improve compatibility with the location of transverse reinforcement. The shear force envelope may be shifted with distance a_l determined in Equation (4).[9,11] The length of the shift depends on the angle of compression strut θ_w of the web truss. The lower angle value is, the larger the shift is. The effect of the shift rule on the cantilever beam shear envelope is presented in Figure 2. It shall be distinguished that same kind of shift, which amount depends on the angle of transversal compressive struts, occurs also in the flange. This shift cannot however happen without transverse reinforcement of the flange and because of that this shift cannot be considered in full when defining where to place transverse reinforcement.

$$a_l = \frac{z^* \cot\theta_w}{2} \tag{4}$$

where θ_w is the vertical compressive struts in the web (Figure 1).

A more detailed TM can be used to determine non-constant σ_y distributions along the web-flange junction.[5,11,14,17] In the tension flange TM, special attention must be given to the end region of the truss. In approaches presented by Bachmann et al., concentration of transverse steel at the cantilever beam end is especially needed when the tension flange does not have a considerable overhang (see Figure 3) beyond the cross section of zero moment.[5,11,14,17] A fitted TM proposed for the test beams of this research is presented in Section 5.6.

3 | EXPERIMENTAL STUDY

The objective of the experimental program was to study longitudinal shear at the web-flange junction in the tension flange of four prestressed beams made continuous. The continuity connections hogging moment capacity and ductility were also studied for the same test beams. The results of the negative bending capacity tests are presented by Kytölä et al.[1]

3.1 | Specimens and loading setup

Each test specimen consists of two 3-m-long prefabricated prestressed concrete rectangular (BxH = 280 × 480 mm^2) beams, which were connected in the laboratory by a transversal diaphragm and longitudinally reinforced deck slab (bxh = 1500 × 120 mm^2). The composite action between precast beams and the in situ cast deck slab was secured with U-shaped stirrups (H1, #10, c/c = 50 mm) and a rough contact surface. Top surface of the precast beams had at least 3 mm roughness at about 40 mm spacing, achieved by raking. Prestressed beams were embedded to the diaphragm by 200 mm. The completed test beams were 6.25-m-long cantilever T-beams, and their aim was to be an isolated model of a half-scale, heavily loaded parking deck structure's intermediate support area.

The nominal dimensions and reinforcement of the test beams are shown in Figure 3. All the deck slabs of the tested beams had identical longitudinal and transversal (#16 c/c 100 mm) reinforcement. The longitudinal reinforcement ratio was high (ρ = 5.9%) and the established transverse reinforcement ratio was selected so that the theoretical load, predicted with Equation (3), of the beam causing web-flange longitudinal shear failure is greater than the load that causes bending failure, regardless which θ_f value was selected from the recommended range. Prestress force and reinforcement of the precast beams varied but it did not considerably influence longitudinal shear of the web-flange junction. Precast beam parts of one of the test beams did not have any prestress force. Remaining three test beams had four to twelve bottom strands and two top strands. All strands were straight throughout the girder length. Prestress at launching was 1350 MPa. Additional information (not vital for this study) about the test beams is presented by Kytölä et al.[1]

Four test girders were tested in negative bending over a central support. The loading points were over the web at both ends of the cantilever beam. The support was directly under the diaphragm column, simulating the action of hogging moment in a continuous composite beam. Load was applied with a hydraulic jack over the web until failure occurred at the compression side of the beam near the support. The system was load controlled and the used loading rate was 50 kN/min. In every load step, visible cracks of the flange slab were highlighted with a marker pen.

3.2 | Material properties

The mean cylinder strength of the precast girder's concrete was 72 MPa, and for the deck and diaphragm

55–57 MPa. Maximum aggregate size for both slab and beam concrete was 16 mm. Compaction of the concrete was conducted by vibration. The cast-in-place deck was covered with plastic film for about 30 h after casting. The increase of the strength of the deck concrete was followed with 14 field cured cylinders ($d = 150$ mm, $h = 300$ mm), and the strength was tested at the time of each loading. The measured concrete cylinder strengths and loading ages of the decks are presented in Table 1. The material properties of reinforcements are given in Table 2.

3.3 | Instrumentation

The flanges of the test beams were divided into three critical cross sections called A ($x = 0$), B ($x = 1235$ mm), and C ($x = 2200$ mm), which were measured. Nine strain gauges (SGB-A1, A2, A3, B1, B2, B3, C1, C2, C3), three per each critical cross section, were attached to the longitudinal reinforcement on one side of the flange to measure strain distribution along the flange. In addition, two strain gauges (SGB-B4, C4) were arranged on the transverse reinforcement located on the flanges at the web-flange junction of cross sections B and C. Figure 4 presents the concrete casting moment of the flange parts of the test beams. The positions of the instrumented cross sections A, B, and C are highlighted.

The in-plane load–deformation response of the reinforced concrete flange at cross-sections B and C was measured with measurement frames (Figure 5). The frames consisted of six diverging displacement sensors (DG-B1–B6, C1–C6), with the aim being to measure average in-plane strains in cracked flanges at the point of cross sections B and C (measured area 700×700 mm^2). The measured area was wide enough to include a few cracks, so that the measured data could be compared to the calculated average values presented in Section 5.8. Not all the results of the measurement frames could be utilized, and the reasons for that are explained in Section 5.2. The location and nomination of instrumentation of the test beams is presented in Figure 6.

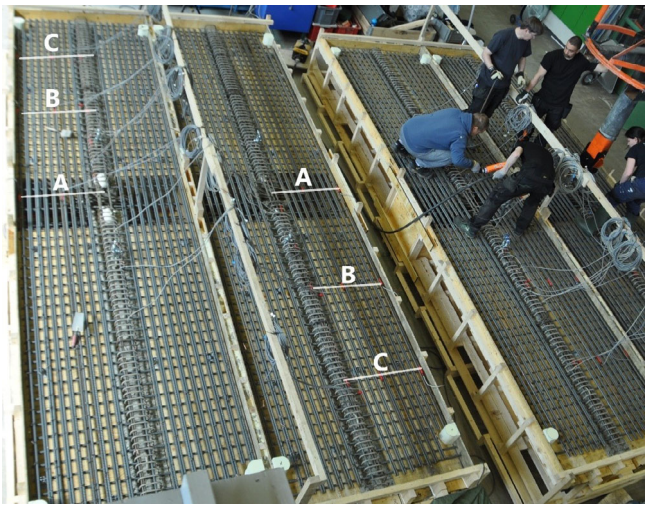

FIGURE 4 Flange reinforcement of test beams and instrumented cross sections A, B, and C

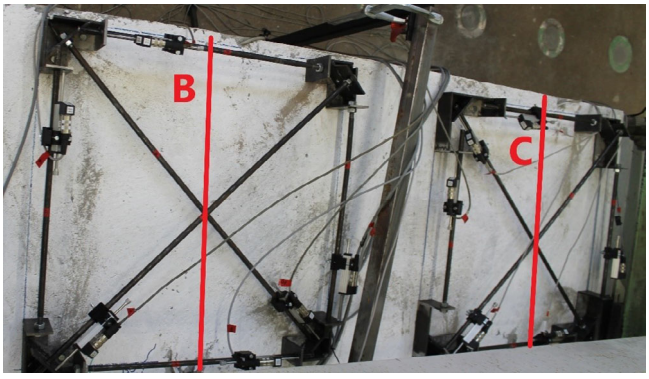

FIGURE 5 Measurement frames measuring in-plane deformations at six directions per section

TABLE 1 Deck concrete properties

Test No.	Slab/diaphragm age at loading (days)	Mean f_{cm} (MPa)
Test 5	23	54.9
Test 6	27	55.9
Test 7	30	56.6
Test 8	34	57.4

TABLE 2 Reinforcement material properties according material certificate

Type of reinforcement	Modulus of elasticity E_s (GPa)	Yield strength f_y or $f_{p0.1k}$ (MPa)	Nominal area (mm^2)	Tensile strength/upper yield strength R_m/R_{eH}	Elongation at maximum force A_{gt} (%)
B500B T16	200	547	201	1.167	12.5
Y1860S7-12.5	192	1813	93.2	1.065	6.0

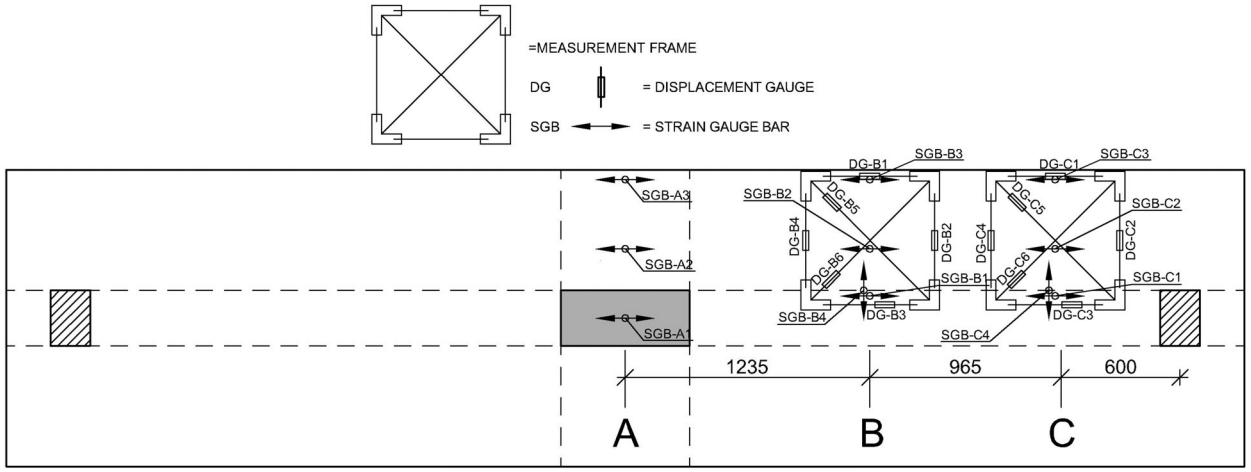

FIGURE 6 Location of measurement frames and strain gauges on flange longitudinal and transversal reinforcements

TABLE 3 The modified compression field theory (modified from Bentz[20])

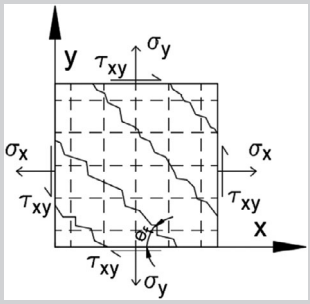

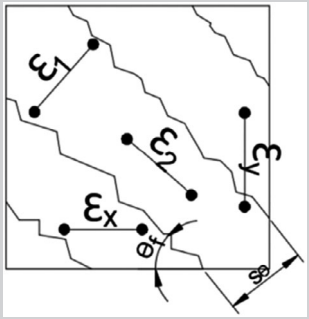

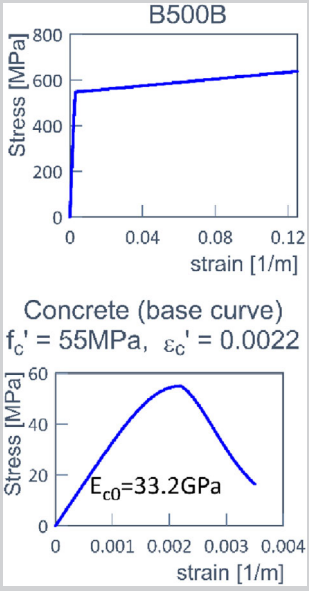

Equilibrium

Average stresses:

$$\rho_x f_{sx} = \sigma_x + \tau_{xy}\cot\theta_f - f_1$$

$$\rho_y f_{sy} = \sigma_y + \tau_{xy}\tan\theta_f - f_1$$

$$f_2 = \tau_{xy}\left(\tan\theta_f + \cot\theta_f\right) - f_1$$

Geometric conditions

Average strains:

$$\varepsilon_x = \frac{\varepsilon_1\tan^2\theta_f + \varepsilon_2}{1+\tan^2\theta_f}$$

$$\varepsilon_y = \frac{\varepsilon_2\tan^2\theta_f + \varepsilon_1}{1+\tan^2\theta_f}$$

$$\gamma_{xy} = \frac{2(\varepsilon_x - \varepsilon_2)}{\tan\theta_f}$$

$$\tan^2\theta_f = \frac{\varepsilon_x - \varepsilon_2}{\varepsilon_y - \varepsilon_2}$$

Average stress—Average strains relationships:

Reinforcement:

$$f_{sx} = E_s\varepsilon_x \le f_{x,\text{yield}}$$

$$f_{sy} = E_s\varepsilon_y \le f_{y,\text{yield}}$$

Concrete:

$$f_2 = \frac{f_c'}{0.8+170\varepsilon_1}\left(2\frac{\varepsilon_2}{\varepsilon_c'} - \left(\frac{\varepsilon_2}{\varepsilon_c'}\right)^2\right)$$

$$f_1 = \frac{f_{cr}}{1+\sqrt{500\varepsilon_1}}$$

$$f_{cr} = 0.45\left(f_c'\right)^{0.4}$$

Stresses at cracks:

$$\rho_x f_{sxcr} = \sigma_x + \tau_{xy}\cot\theta_f + v_{ci}\cot\theta_f$$

$$\rho_y f_{sycr} = \sigma_y + \tau_{xy}\tan\theta_f - v_{ci}\tan\theta_f$$

Crack widths, w:

$w = s_\theta\varepsilon_1$, where

$$s_\theta = \frac{1}{\frac{|\sin\theta_f|}{s_{mx}} + \frac{|\cos\theta_f|}{s_{my}}}$$

s_{mx}, s_{my} = stabilized crack spacing estimates in x and y directions

Allowable shear stress on crack

$$v_{ci} \le \frac{0.18\sqrt{f_c'}}{0.31+\frac{24w}{a+16}}$$

a = maximum aggregate size

4 | COMPUTATIONAL ANALYSIS

The design of reinforced concrete elements subjected to significant shear is a complex engineering problem. Generally used design approaches presented in Section 2 predict the shear strength of the flange based on the TM and CBT. When it comes to the longitudinal shear capacity of the web-flange junction, the literature has highlighted the poor accuracy of these approaches in some situations compared to experimental results.[10,17] More sophistication can be applied in evaluating longitudinal shear by applying a nonlinear analysis of the compression field theory.[18]

An expressive but relatively complex nonlinear analysis method called the modified compression field theory (MCFT) was developed in the 1980s. It is able to predict more accurately the full load deformation relationships and shear strength for membrane elements subjected to in-plane shear and normal stresses. In the model, cracked concrete is treated as a new material with its own stress–strain relations. Equilibrium, compatibility, and stress–strain relationships are formulated in terms of average stresses and average strains. The model takes into account tensile stresses in the concrete between the cracks.[19] Table 3 summarizes the MCFT for the two-dimensional case studied in this paper.

Membrane-2000, a structural software program developed by Bentz, conducts the nonlinear sectional analysis for reinforced concrete shells that are subjected to in-plane forces N_x, N_y, and N_{xy} and models its full load–deformation relationship based on MCFT, as presented in References 19–21. In this study, the computational MCFT examinations have been conducted with Membrane-2000.[22]

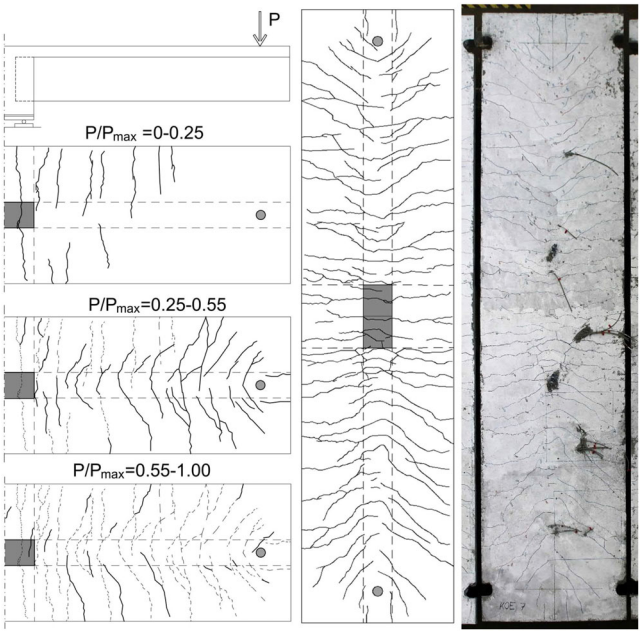

FIGURE 7 Cracking of the tension flange of test beam 7

TABLE 4 General results of load tests

Test No.	P_{max} (kN)	M_{max} (kNm)	M_y (kNm)
Test 5	750	1999	$0.66M_{max}$
Test 6	764	2014	$0.75M_{max}$
Test 7	767	2024	$0.66M_{max}$
Test 8	795	2096	$0.63M_{max}$

5 | RESULTS AND DISCUSSION

5.1 | Observations from loading tests

Few thin cracks were observed at the slab part of the test specimens prior to the loading, most likely caused by differential shrinkage between the deck and the precast beam. Until the load level reached ~25% of the failure load more transverse cracks appeared in the slab at the support area. Inclined cracks caused by longitudinal shear were shown at the load level of 25–55% of the failure load. The pattern of cracking of the flange plate was fixed at a load level of 55% of failure load and did not change with increasing load. Cracks at the support area were perpendicular to the beam's longitudinal axis, almost parallel to this axis at the end of the cantilever beam and between them with correspondingly changing inclination. The crack patterns of the test beams showed clear signs of longitudinal shear effects. Tension flange crack patterns of test beam number 7 are presented in Figure 7. The figure presents crack formation at different load levels and the final crack pattern. The pattern of test 7 is similar to that found in tests 5, 6, and 8.

The selected combination of longitudinal and transverse reinforcement in the test beams was sufficient to control the longitudinal cracking in the web flange junction and ensure the integrity of the section. According to visual observations, none of the tested beams reached longitudinal shear failure in the web-flange junction. It was also found in all the tests that the horizontal plane of the junction remained undamaged.

The observed failure mode of the test beams was flexural failure. Failure of all test beams was clearly controlled by tension, and extensive yielding of the longitudinal deck reinforcement was evident over the support before the crushing of the composite beam's soffit concrete. The vertical deflections of the cantilever beam ends were considerable prior to the failure (L/32–L/17).[23] According to strain gauge bar measurements (SGB-A1,

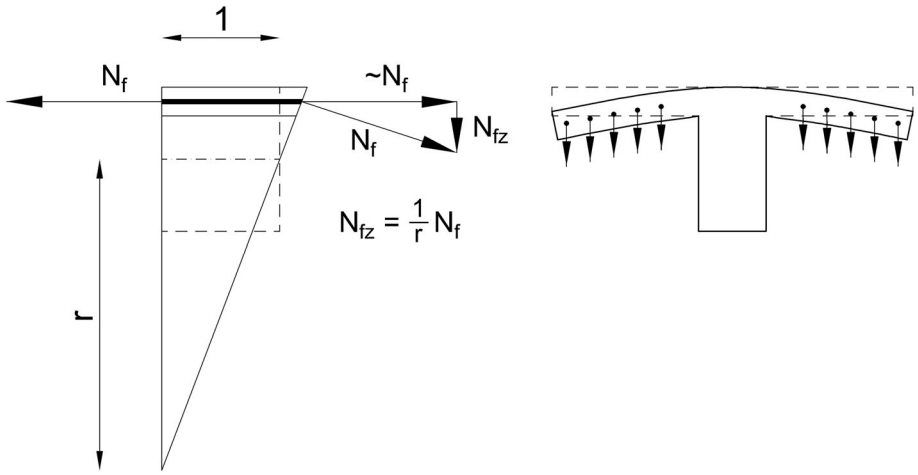

FIGURE 8 Bending of a flange due longitudinal curvature of a beam (modified from Jonasson[24])

A2, A3), the deck part's first longitudinal reinforcement yielded over the support's center line at a load level of 63–75% of failure load. After that, a plastic hinge started to form and its length extended to 400–800 mm away from the edge of central support. Detailed information about the test beam's negative flexural bending capacity is published by Kytölä et al.[1]

Table 4 summarizes the loading capacities of the test beams. It shows the maximum cantilever load P_{max} and the maximum experimental bending moment M_{max} over the support ($x = 225$ mm) of all tested beams. Table 4 also shows the relative tested negative bending moment at the onset of first yielding of top reinforcement over the intermediate support. Self-weight of the test beam and the weight of loading equipment are included in the values presented in Table 4.

5.2 | Transverse bending due to longitudinal curvature

Measurement frames (DG-B1–6 and DG-C1–6) 30–100 mm above slab top surface (presented in Section 3.3) were intended to measure in-plane deformations of cross sections B and C caused by shear and axial stresses. The measurement frames yielded measuring data for four directions at six locations, which would have been sufficient for defining the average main strains and angle of compression spread of the elements. From the crack pattern, it was concluded that the diagonal rods of the measurement frames were approximately in the direction of the main strains. One diagonal rod measured roughly the main compression strain and the other the main tension strain. However, according to the measuring data both diagonal rods were in tension.

A feasible explanation for these results is the transversal bending of the flange overhang due to the beam curvature (flange-curl phenomenon) combined with high eccentricity of the displacement sensors in measuring frames. The flange-curl phenomenon has been discovered in several earlier experimental studies. Previous research has established that, even if no loads are applied at the web-flange outstands, transverse moments are produced at the web-flange junctions when a beam develops longitudinal curvature (see Figure 8). Though this flange-curl phenomenon is not a major effect, appreciable vertical deflections of unloaded flange outstands have been recorded in many tests.[5,17,24,25] The tested cantilever beams exhibited high longitudinal curvature values which are presented by Kytölä et al.[1]

Experimental results of the measurement frames indicate that some transverse deflections were also observed in these tests. Because of transverse deflections, only the shear strain of the measured cross sections B and C could be reliably determined according to the measurement frames DG-B5–6 and DG-C5–6. Other data gained from the frames were not utilized in this study. The shear strain data of these measurements are used in the results presented in Section 5.8. For simplification, flange-curl phenomenon is disregarded at computational analysis made in following sections.

5.3 | Flange longitudinal strains

Flange longitudinal reinforcement strains were measured at cross sections A, B, and C. In every cross-sectional longitudinal strain was measured from three points (1: over the web, 2: $y = 360$ mm, and 3: $y = 720$ mm). This information was useful when verifying if the whole flange width was effective during loading.

Figure 9 represents the flange longitudinal reinforcement strain and stress profile for different load levels across flanges at three different cross-sections. The

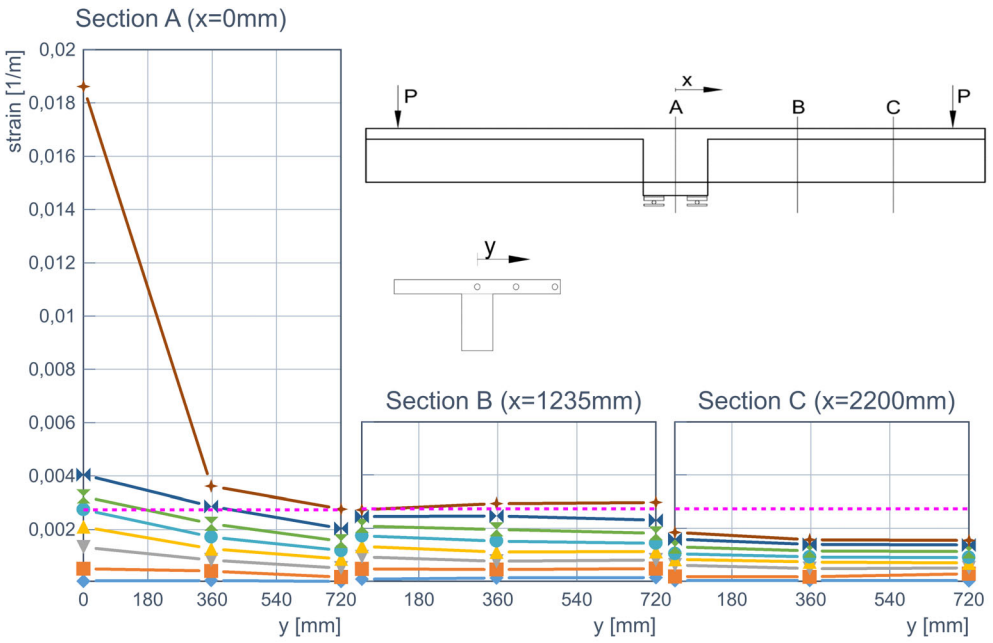

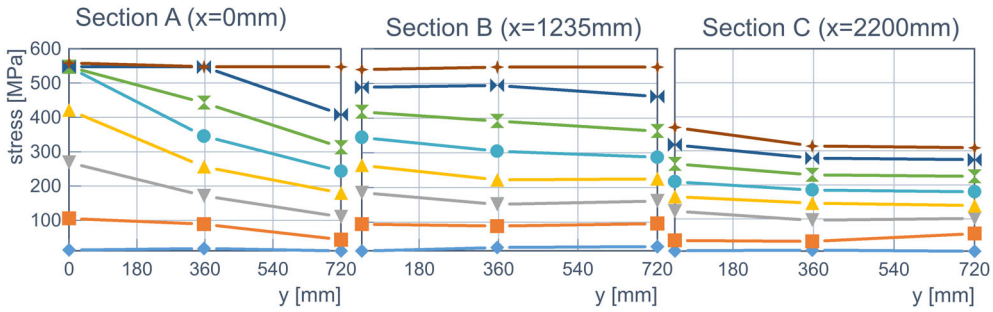

FIGURE 9 Longitudinal strain and stress distribution in the reinforcing bars of test beam 7 across the flange at locations SGB-A1–3, -B1–3, and -C1–3 and different values of load

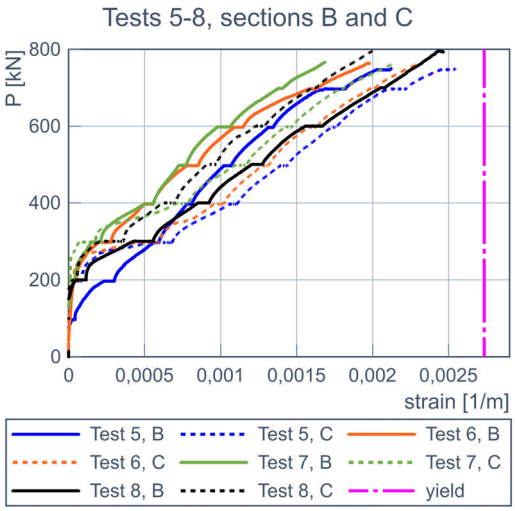

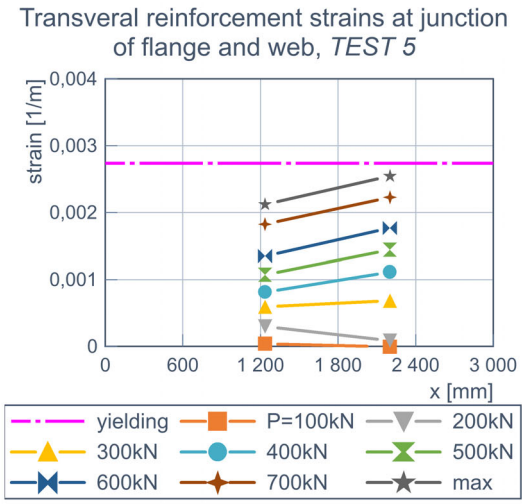

FIGURE 10 Flange transversal strain diagrams according to strain gauge measurements from transverse reinforcement SGB-B4 and SGB-C4

presented case reflects the general behavior of all tested beams.

Cross section A: Nonuniform bending stresses and strains across the flange width were observed. Strains over the web were higher than those of the reinforcement remote from the web. As the load level increases to near failure, reinforcement reaches the yield limit and the stress profile turns into uniform. The strain profile,

however, is unevenly distributed during the whole loading test. At the maximum load level, strains over the web increased considerably.

Cross section B: Both the stress and strain profiles were uniformly distributed. The whole flange width was effective from start to finish. Reinforcement reaches the yield limit at the end of the loading test.

Cross section C: Both the stress and strain profiles were uniformly distributed. The whole flange width was effective from start to finish. Maximum stress level reached at failure was approximately 60% of the yield strength.

Some national design specifications and data from experimental studies suggest that shear lag of composite T-beams could be neglected at ULS on the basis of concrete cracking and reinforcement yielding, allowing stresses to redistribute across the flange.[11,26,27] Conflicting experimental results have also been published, according to which a reduction in effective width value was observed as the load level increased.[18,28] Effective width at intermediate support increases as the loading proceeds if observed from stress distribution, on the other hand strain distribution indicates effective width reduces. EN 1992-1-1 uses the same effective width for both SLS and ULS.[9,11]

5.4 | Flange transverse strains

Flange transverse strains were measured with strain gauges in the transverse reinforcement at cross sections B and C (SGB-B4, SGB-C4 at Figure 6). Figure 10 represents the transverse strain values at different tests and load steps. Transversal strains of the reinforcement are insignificant up to a load level of approximately $P = 200$ kN, apart from the strain result of Test 5 cross section B. According to the crack patterns presented in Figure 7, longitudinal shear cracking took place also at the same load level. After that, transversal strains begin to increase. The leaps seen in the strain–load relation are due to the load increase were stopped in order to observe deck cracking at every load step. Strains at location C were greater compared to cross section B and the distribution increased toward the cantilever end, except in Test 8 where the strains at cross section C were minor. Transverse reinforcement did not yield, but the strains were high, reaching 62–93% of the yield strain.

Due to lack of space, used transverse reinforcement were straight bars without any hooks at the ends. From the design specification viewpoint, the anchorage conditions of these bars were not complete. Despite of this test, results indicate that transversal reinforcement worked properly, and the anchorage was adequate.

5.5 | Web-flange longitudinal shear stress τ_{xy} distribution

An analytical approach is used to evaluate longitudinal shear stress distribution at the web-flange junction from the intermediate support to the tip of the cantilever beam. According to Equation (1) and Figure 1, shear stress can be determined from the change of the normal force in the flange. Reinforcement strains of the tested tension flange are measured at cross sections A, B, and C. The bending moment at the tip of the cantilever is null and the normal force of the flange is assumed to be null at the end of the deck's longitudinal tension reinforcement. For the estimation of axial normal force N_{fx} along the beam in the flange, results of strain gauge bar measurements (SGB-A1–3, -B1–3, and -C1–3, see Figure 6) were used. From these measuring points, three ΔN_{fx} values (the change in longitudinal force in the flange) could be determined (at regions A-B, B-C, and C-Tip of the cantilever). The reinforcement stress–strain relation presented in Table 3 was used to convert the strain gauging to stress distribution. Tension resultant force N_{fx} could be determined by integrating tension stress into the flange. This methodology has uncertainties because it

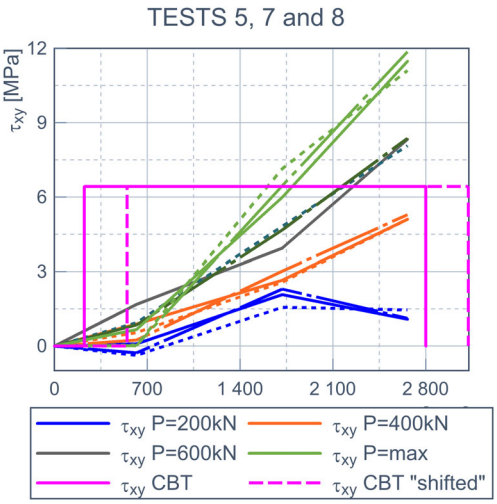

FIGURE 11 Shear stress distribution along beam length at different load levels

TABLE 5 Flange overhang normal forces

Test 8	N_{fxA} (kN)	N_{fxB} (kN)	N_{fxC} (kN)
$P = 200$ kN	343	384	118
$P = 400$ kN	939	905	555
$P = 600$ kN	1545	1420	879
$P = 795$ kN (max)	1996	1993	1245

takes into account only reinforcement stresses and does not consider concretes contribution to the tensile force. Due to limitations of experimental data, the influence of residual tensile stresses in the cracked concrete and aggregate interlock cannot be included to the presented experimental results. Closely spaced crack patterns presented in Figure 7 and minor variation between experimental results shown in Figure 11 might be related to that these possible sources of error are not significant near the final load level of the specimen.

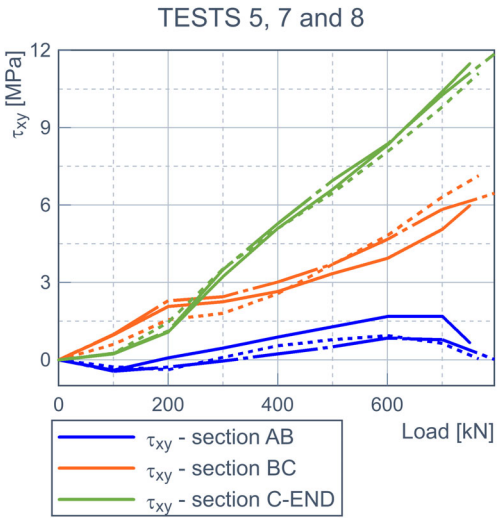

FIGURE 12 Shear stress at cross sections AB, BC, and C-END during loading

Table 5 shows normal forces of the flange overhang at cross sections A, B, and C of test beam 8 at different load levels. It can be seen from the table that the change in the normal force between cross sections A and B is insignificant. On the other hand, normal force at cross section C is considerable, taking into account that the section is only at a 600 mm distance from the loading point.

Measured longitudinal shear stress distributions at the junction between one side of the flange and the web of all tested cantilever beams are presented in Figure 11. The results of test 6 are not presented because one relevant gauge bar was damaged and hence its shear distribution could not be evaluated. Elastic and shifted calculated shear stress distributions based on CBT presented in Section 2.1 are also implemented to the figure. What stands out from the tested shear distribution is

1. Shear stress at between cross sections A and B (=AB) is negligible during loading and zero at the maximum load where the reinforcement is yielding in both sections.
2. The shape of the shear stress distribution changes during loading. These changes may partly be explained by the fact that methodology used to determine experimental shear stress does not take concrete tensile stresses into consideration.
3. At the maximum load, shear stress concentrates more under the loading point and the shape of the distribution is triangular rather than a square

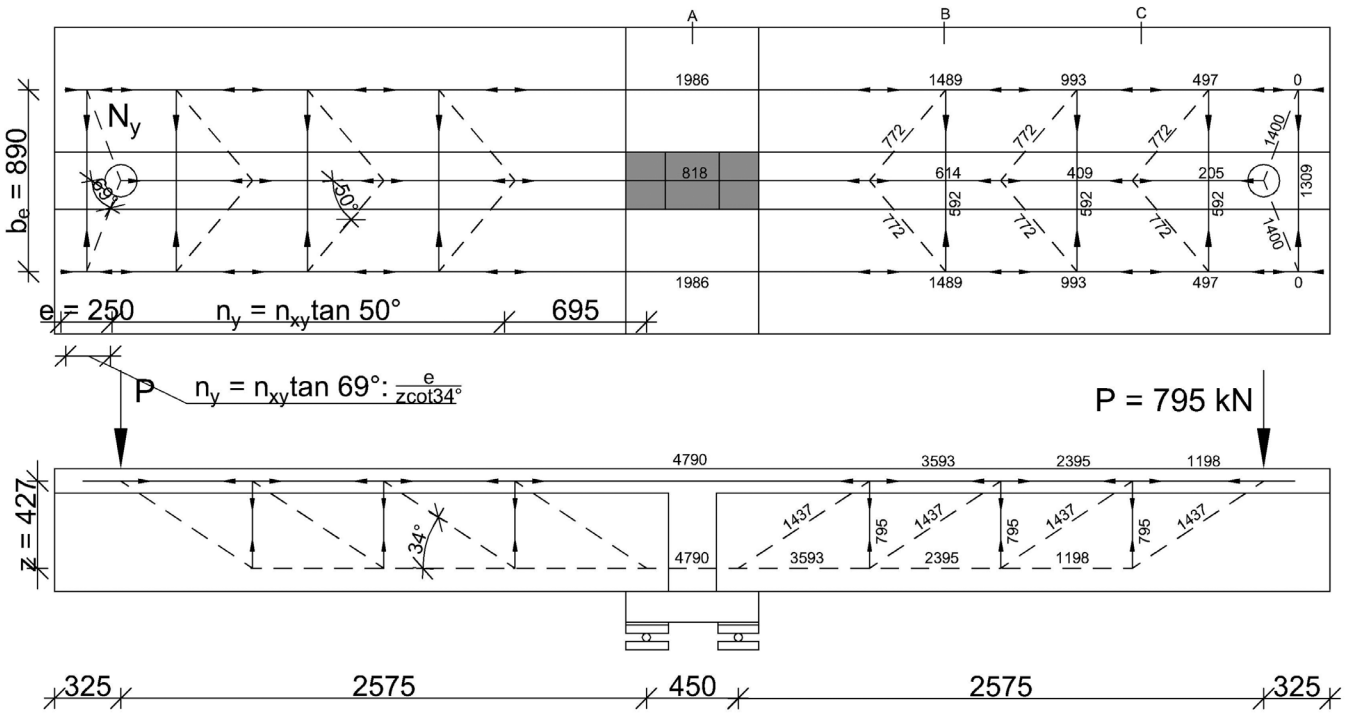

FIGURE 13 Truss model for test beam 8. Longitudinal flange reinforcement outside the web treated as two units

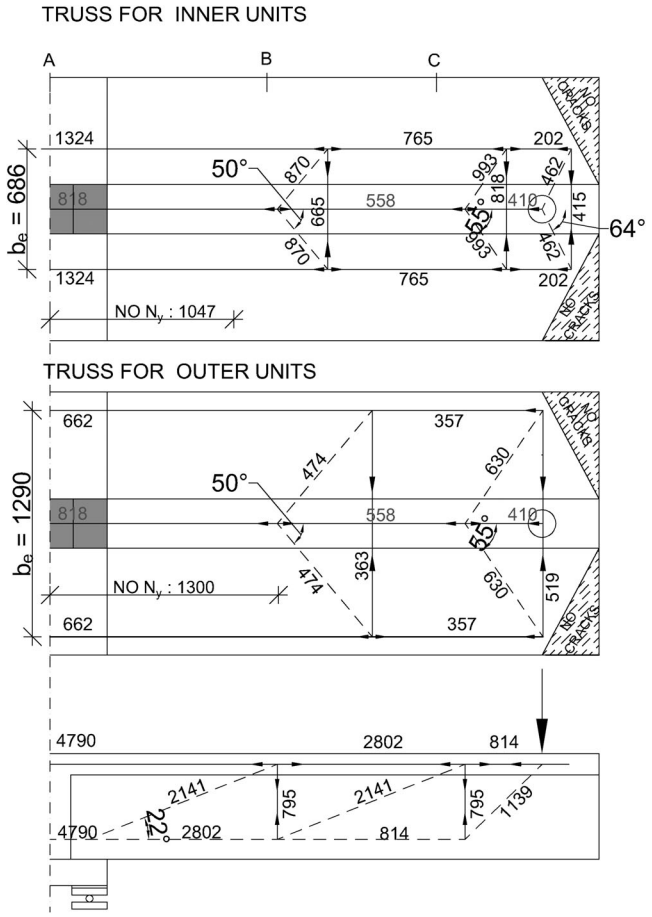

FIGURE 14 Truss model for tested tension flange of test beam 8. Longitudinal flange reinforcement outside the web treated as four units (inner and outer). Total N_y is the sum of inner and outer transversal forces

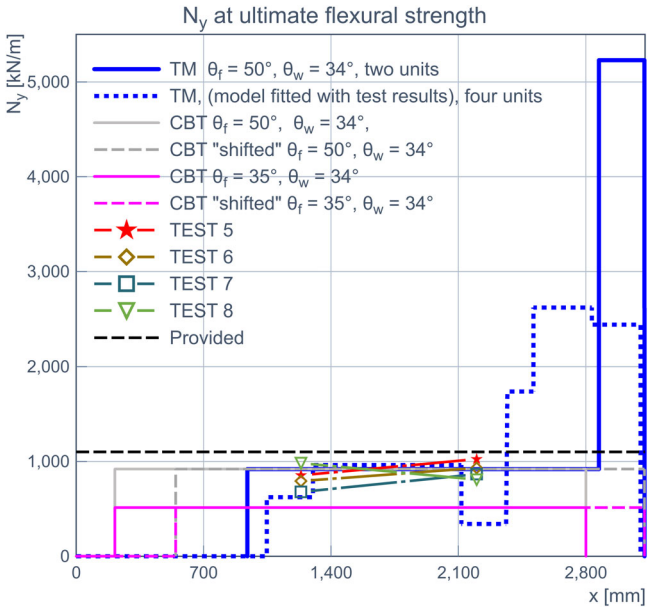

FIGURE 15 Calculated and tested force per unit length in the transverse reinforcement (SGB-B4 and C4) in the tested cantilever beam. Maximum vertical load of test beam 8 used in the calculated distributions

4. Maximum measured shear stress near the loading point is almost double compared to the value defined according to CBT.

Figure 12 presents redistribution of the shear stress between different cross sections during loading. The test setup is an isolated part of a complete continuous structure. It is important to bear in mind the possible bias between these two structures. Direct conclusions of shear stress distribution of a continuous girder cannot be drawn from the results of this study.

5.6 | Transversal force N_y at web-flange junction

CBT avoids the need to construct a TM, and the required transverse reinforcement per unit length can be determined in accordance with Equation (3). The equation is based on the smeared TM, where the struts and ties are not discrete.

Figure 13 presents the test beam's TM, which deals with the shear flow for a complete beam on the basis of pure truss actions. Compared to the beam theory described above, it has the advantage of taking into account the distribution of shear along the web-flange junction. Overhang beyond the section of zero moment is dealt with the adjusted truss angle in the end zone (increased θ_f) to adapt the truss to the length available for the dispersion of forces across the flange. The procedure was proposed by Bacchetta and Bachmann.[15,17]

Figure 13 treats the longitudinal reinforcement outside the web as two units, one in each flange outstand. Full effective flange breadth is also presumed. The longitudinal reinforcement ratio of the test beams was also kept the same for the full length of flange. When the whole flange breadth is not required for flexural resistance, the method presented in Figure 13 may lead to unnecessary demands for transverse flange reinforcement. A more detailed model about flange truss is presented in Figure 14, where reinforcement outside the web is divided into four units. The force in the tension units along beam length is tailored with measured strain distributions presented in Figures 9 and 10. Adapted TM at Figure 14 takes also into consideration measured compression angle values of the flange presented at incoming Section 5.7. Flange corners at the end of

the cantilever tips without concrete cracking were presumed to be not effective. Also, this model is clearly a simplification, but it does however lead to more evenly distributed transversal reinforcement and does make it clear that the decrease of longitudinal steel forces with decreasing bending moment is far slower than implied by the simplification (m/z).[25]

To illustrate how the force in the transverse reinforcement required by the presented methods (CBT and TM) compares with the corresponding measured values in cross sections B and C in the loading test, Figure 15 shows the variation of this force along the flange-web connection of the test beam. The shifting of the N_y diagram, determined according to CBT, is explained in Section 2.2. The strength of the provided constant transverse steel (Ø = 16 mm, c/c = 100 mm) in the flange is also presented.

The tested N_y is obtained by multiplying the area of the transverse steel per unit length of the connection by its maximum stress. Obviously, tested N_y cannot exceed the strength of the provided reinforcement. However, if the yield limit of the provided transversal reinforcement is reached, it indicates the need for more reinforcement to improve serviceability.[10]

The provided reinforcement exceeds the reinforcement area of CBT. None of the tested transversal

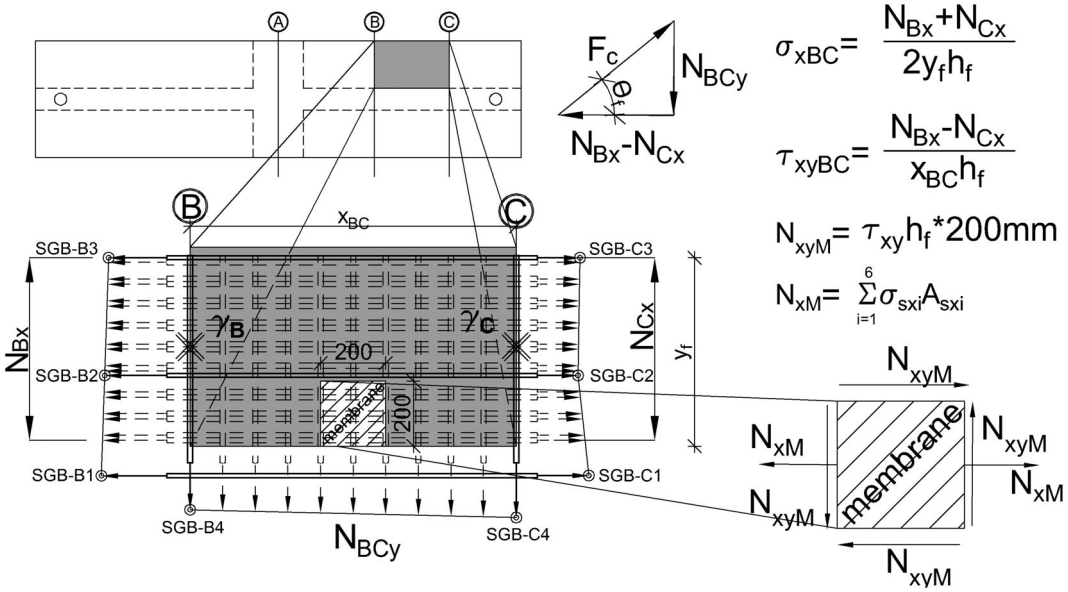

FIGURE 16 Method to define angle Θ_f according to test results. The results are presented in Figure 17

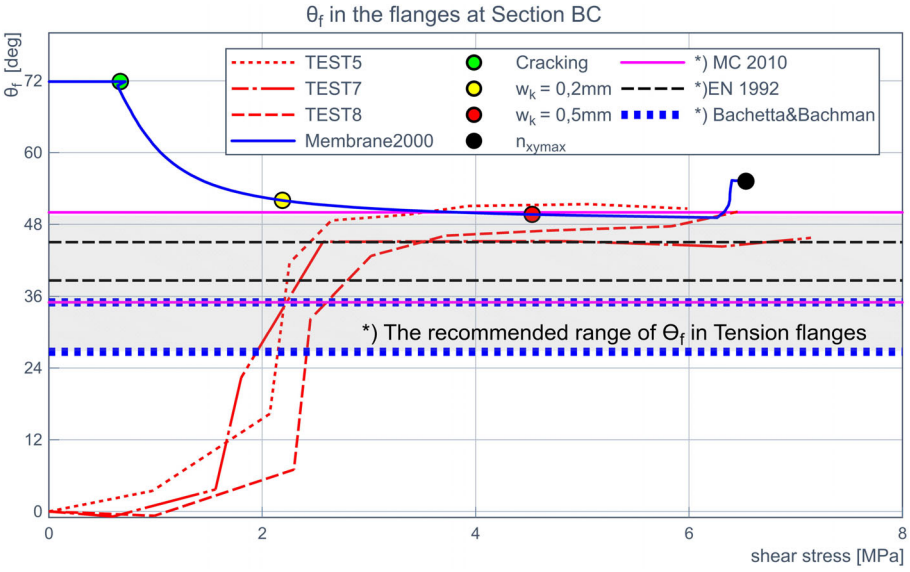

FIGURE 17 Calculated and measured angle Θ_f between the concrete compression strut and the web's longitudinal axis

reinforcement yielded, but the force in them was greater than CBT predicted with low Θ_f values. According to the TMs provided, transverse reinforcement at flange overhang beyond zero bending moment was inadequate.

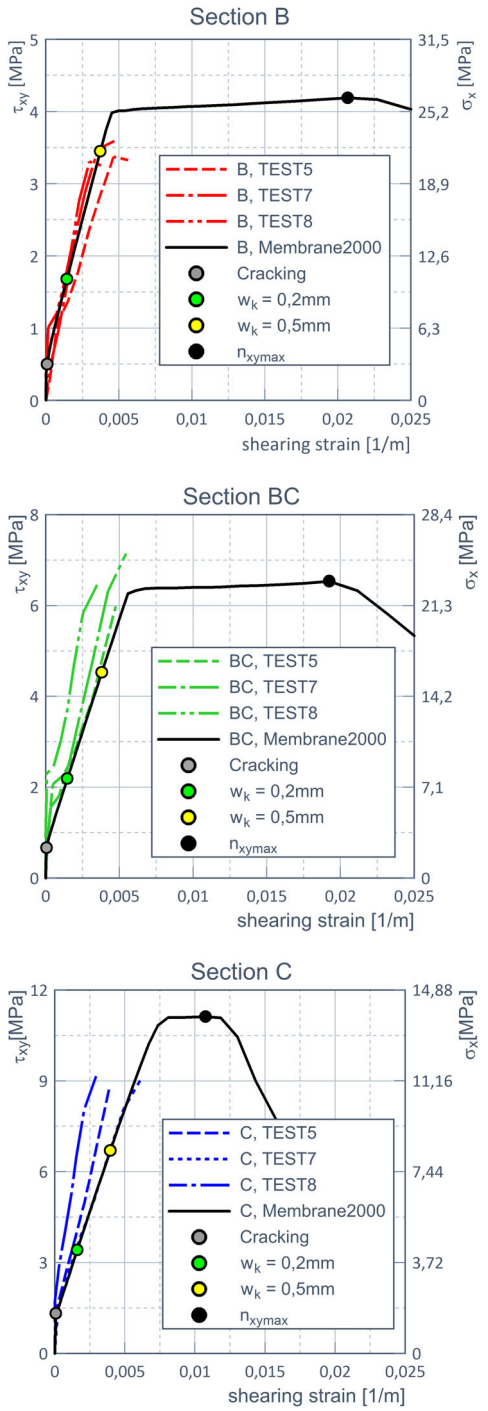

FIGURE 18 Tested and calculated shear stress-shear strain relation at cross sections B, BC, and C

Shear stress distribution presented in Figure 11 also indicates that concentrated transversal reinforcement would have been needed at the end region of the test beam. Unfortunately, transversal strain measurement was not made at the end of the cantilever tip.

5.7 | Θ_f in the test beam's tension flange

In order to determine angle Θ_f between the concrete compression strut and the web's longitudinal axis, a ~1-m-long part of the tested deck slab on the other side of the web between cross sections B and C was studied separately. Shear, longitudinal and transversal strains were measured at cross sections B and C. With the help of measured data and the TM, the relation of the mean angle Θ_f and shear stress between cross sections B and C could be evaluated at a cracked state. The method used is presented in Equation (5) and Figure 16.

$$\theta_f = \arctan\frac{N_{BCy}}{N_{Bx} - N_{Cx}} \tag{5}$$

The studied element is subjected to axial resultant forces N_{Bx} and N_{Cx} in x direction and longitudinal shear N_{xy} at the junction of the flange and the web. As a result, transversal reinforcement becomes active. The relation between shear stress and the angle of the compression strut at the junction of the web and the flange was analyzed with Membrane-2000 (presented in Section 4). The 200 × 200 mm^2 membrane element which is subjected to in-plane forces N_{xM} and N_{xyM} between cross sections B and C at the junction of the web and flange was cut out and studied. The ratio between two loads acting on the element's edge planes of the studied membrane element could be determined at a cracked state with the help of measured σ_{xBC} and τ_{xyBC} (Figure 16). The value of N_{xM} used in the analysis was determined according to six reinforcement bars that were nearest to the web-flange junction. The relation of the loads, determined with the method described above, reached a constant value after cracking stress was exceeded in all tests at the load level of 35% of maximum load which means that at section BC while shear stress is lower than ~2.5 MPa concretes contribution to the shear capacity is considerable. After the shear stress reached the value 35% of the maximum load (=2.5 MPa) for the studied element BC, the relation of

TABLE 6 Summary of loading ratios of studied cross sections

	B (x = 1235 mm)	BC (x = 1718 mm)	C (x = 2200 mm)
N_{xyM}/N_{xM}	0.159	0.282	0.807

N_{xyM}/N_{xM} varied between 0.25 and 0.32 at different tests. Mean value $N_{xyM}/N_{xM} = 0.28$ was used in the computational analysis.

Both calculated and tested angle relation to shear stress are presented in Figure 17. At the beginning of the loading, the measured angle value is zero, whereas calculated Θ_f starts from value 72°. The difference of the curves at the beginning of the loading is the consequence of the method to evaluate the tested angle. The procedure is based on the strut-and-tie model which does not take the contribution of concrete into consideration. The defined angle value determined this way is not relevant until the concrete has cracked. The curves can be divided into three separate development stages:

1. $\tau_{xy} = 0$–1 MPa: According to the calculated result, the angle is large and feasible cracks are nearly perpendicular to the beam axis. Concrete reaches its peak tension stress at the sharp inclination change of the curve and the first cracks appear. Tested angle value is zero which is not a valid result. The reason for this inconsistent result is that at this stage force at transversal reinforcement is for the most part nonexistent, which means that shear force is transmitted through concrete.
2. $\tau_{xy} = 1$–2.5 MPa: Both concrete and transversal reinforcement are active, and the angle value changes. Calculated and measured angle values approach each other. Values are still away from each other because the shear stress has not reached 35% of the maximum after which experimental results are valid.
3. $\tau_{xy} = 2.5$–6 MPa: Shear stress and force at transversal reinforcement increase at the same rate, which means that the capacity of concrete is exceeded. In addition to tested and calculated transversal compression angle values, Figure 17 provides an overview of recommended Θ_f range from different references. Both calculated and tested angle values are at the upper bound of the range and are in good agreement.

Previous studies have reached similar Θ_f–τ_{xy} relations for experimentally studied tension flanges.[24]

5.8 | Shear stress τ_{xy}–shear strain γ_{xy} relation

In addition to longitudinal and transversal strains, shear strain was also measured from the tested cross sections B and C (DG-B5–6 and DG-C5–6, Figures 5 and 6). Combining the results from shear strain measurements and the τ_{xy} definition presented in cross section 5.5, the τ_{xy}–γ_{xy} relation could be drawn for cross sections B, BC, and C (see Figure 18). Shear strain at cross section BC was assumed to be the average of values measured from cross sections B and C.

For the computational study, small membrane elements were separated from the junction of the web, and the flange at cross sections B, BC, and C alike was done in the previous paragraph for cross section BC. Relations of τ_{xy}–γ_{xy} were then calculated with Membrane-2000. The ratios between in-plane forces N_{xyM} and N_{xM} subjected to membrane elements were defined in cross sections B and C with the same methods described for cross section BC previously. Loading ratios are presented in Table 6. Information of the development of the cracking of the flange has been added to computational curves.

At cross section B, normal force is dominant compared to shear and the tested and calculated τ_{xy}–γ_{xy} relations are in good agreement. The tested relation seems to reach the maximum shear stress a bit earlier than the calculated curve. When the ratio of shear force increases closer to the cantilever tip, the disparity between calculated and measured relation increases. This inconsistency may be partly due to measurement frames measuring an average shear strain for the whole flange outstanding while the computational results are from the web flange junction. Taking into consideration the variation that the test results have between each other, the calculated estimation made with Membrane-2000 compared to the test results is good. According to the analysis made with Membrane-2000, the further away from the central support the section is the higher the maximum τ_{xy} capacity it has.

6 | CONCLUSIONS

The purpose of the current study was to examine longitudinal shear stress of the web and flange junction at the hogging moment area of a continuous composite T-beam made from separate precast concrete girders and cast-in-place deck slab. Longitudinal shear-stress distribution and transversal strains of the flange were experimentally tested from four half-scale cantilever specimens, and the results were compared to methods found from literature. The conclusions of this study can be listed as follows:

1. One of the more significant findings to emerge from this study is that longitudinal shear distribution between the web and the flange according to CBT is not always at a safe side. A notable difference between analytical and tested longitudinal shear distribution was observed. The magnitude of tested longitudinal shear stress at failure at the end of the cantilever tip

was almost double compared to the value based on CBT, smeared truss and maximum recommended compression angle value.
2. Both experimental and analytical findings suggest that the cantilever beam requires concentration of transverse steel at the beam end. The computational examples made with discrete TM showed that simplified methods may, however, lead also to unnecessary demands for transverse flange steel. Required transversal reinforcement at the end part of the tested cantilever beam according discrete TM examples was two to three times greater than provided reinforcement. This requirement seems overconservative taking into consideration that the tested flange did not reach shear failure.
3. The experimentally and analytically determined compression angle value Θ_f at studied cross section BC was about 50°, which is at the upper bound of recommended angle values presented in Model Code 2010. This is much more than the recommended design values ($\Theta_f = 27–31°$) of the highly cited paper by Bacchetta and Bachmann.[15]
4. Between the first yielding of longitudinal reinforcement at the hogging moment area and final failure, the test beams developed a long plastic hinge near the continuity connection. At that stage, shear stresses disappeared along the length of the plastic hinge and concentrated at the cantilever end. Without adequate transversal reinforcement, this redistribution could not been happened, and the failure load and mode of the studied structure might have been different.
5. Flange shear cracking started at a relatively early phase of loading. Conventionally longitudinal shear is considered a ULS phenomenon. Parking deck structures are located at aggressive environmental conditions and have strict cracking width limits. Further investigation and experimentation into cracking caused by longitudinal shear at SLS is recommended.
6. Clear shear lag phenomenon was detected at flange longitudinal reinforcement strains over the support of the tested beams tension flanges. By contrast, at the cross-sectional remote from support, strains were evenly distributed.
7. The MCFT is a convenient method in analyzing the in-plane shear deformation response of the flange of the T-shaped cross section.
8. Experimental study on complete continuous T-shaped composite beams is needed to gain information on web flange junctions longitudinal shear distribution.
9. More research concerning the combined effects of longitudinal shear, transverse bending, and vertical shear on transversal reinforcement of T-beams flange is needed.

ACKNOWLEDGMENTS

The authors gratefully acknowledge the financial support provided by the Finnish concrete industry. The authors would also like to thank Mr Jani Kujala for his assistance in the laboratory phase of this study.

NOTATION

a_l	Reference 9 (9.2)
A_s	total amount of flexural reinforcement area
A_{sf}	part of A_s, placed in one side of the flange overhang
E_{c0}	concrete tangent modulus at stress $\sigma_c = 0$ MPa
F_c	concrete compressive force at Flange
h_f	deck thickness
L	distance between loading point and intermediate support (Figure 3)
σ_x, σ_y, τ_{xy}	stress at specified section and direction (MPa)
N_x, N_y, N_{xy}	force per unit at specified section and direction (kN/m)
N_f	resultant force at specified section and direction (kN)
P	load at cantilever tip during load test
r	radius of curvature
V	shear force of the cross-section
y_f	width of one side of the flange outstand (Figure 3)
z	inner lever arm, corresponding to the bending in the cross section
γ_{xy}	shear strain
ε_x, ε_y	strains at directions x and y
ε_1, ε_2	principal strains
Θ_f	angle between the concrete compression strut and the web's longitudinal axis at flange
Θ_w	angle between the concrete compression strut and the beam's axis at web
ρ	geometric reinforcement ratio A_s/bd
v_{ci}	shear stress on the crack at MCFT analysis
ρ_x, ρ_y	reinforcement ratio for x and y directions

DATA AVAILABILITY STATEMENT

Data available on request from the authors.

ORCID

Ulla Kytölä https://orcid.org/0000-0003-0645-8146
Joonas Tulonen https://orcid.org/0000-0002-0879-244X
Anssi Laaksonen https://orcid.org/0000-0001-8459-7470

REFERENCES

1. Kytölä U, Asp O, Laaksonen A. Negative bending tests on precast prestressed concrete beams made continuous. Struct

Concr. 2021;1–20:2223–42. https://doi.org/10.1002/suco.202100043
2. Kaar PH, Kriz LB, Hognestad E. Precast-prestressed concrete bridges 1. Pilot tests of continuous girders. J PCA Res Dev Lab. 1960;2:21–37.
3. Miller R, Castrodale R, Mirmiran A, Hastak M. NCHRP report 519. Connection of simple-span precast concrete girders for continuity. Washington, DC; Transportation Research Board; 2004.
4. Newhouse CD. Design and behaviour of precast. Prestressed girders made continuous—an analytical and experimental study. Blacksburg, Virginia: Virgiana Polytechnic Institute and State University; 2005.
5. Eibl J, Kühn HE. Versuche an Stahlbetonplattenbalken mit gezogener Platte. Beton und Stahlbetonbau. 1979;74(7):176–81. https://doi.org/10.1002/best.197900290
6. Leonhardt F, Mönning E. Vorlesungen über Massivbau, Dritter Teil: Grundlagen zum Bewehren im Stahlbetonbau. Berlin: Heidelberg, New York; 1976.
7. Regan PE, Placas A. Limit-state design for shear in rectangular and T beams. Mag Concr Res. 1970;22(73):197–208.
8. EN 1992-2. Eurocode 2: design of concrete structures. Part 2: concrete bridges. Design and detailing rules; 2005
9. EN 1992-1-1. Eurocode 2: design of concrete structures. Part 1–1: general rules and rules for buildings; 2005
10. Razaqpur AG, Ghali A. Design of Transverse Reinforcement in flanges of T-beams. J Am Concr Inst. 1986;83(4):680–9. https://doi.org/10.14359/10662
11. Hendy CR, Smith DA. Designers' guide to EN 1992-2, Eurocode 2: design of concrete structures. Part 2: concrete bridges. London: Thomas Telford Publishing; 2007.
12. Tizatto V, Shehata LCD. Longitudinal shear strength of wide compression flanges. Mater Struct. 1990;23(1):26–34. https://doi.org/10.1007/BF02472995
13. AASHTO. AASHTO LRFD bridge design specifications; 2012
14. Leonhardt F. Vorlesungen über Massivbau, Sechester Teil: Grundlagen des Massivbrückenbaues. Berlin: Heidelberg, New York; 1979.
15. Bacchetta A, Bachmann H. Versuche über Längsschub, Querbiegung und Quervorspannung in Zugplatten von Betonträgern. Zürih: *ETH Zürich*; 1979. https://doi.org/10.3929/ethz-a-000184909
16. FIB. Fib Bulletin 66, Model Code 2010, Final draft. Vol 2. Lausanne, Switzerland: International Federation for Structural Concrete (fib); 2012.
17. Comite Euro International du Beton. Bulletin d'information N146, shear, torsion and punching; 1982
18. Pereiro-Barceló J, López-Juárez JA, Ivorra S, Bonet JL. Experimental analysis of longitudinal shear between the web and flanges of T-beams made of fibre-reinforced concrete. Eng Struct. 2019;196-(June):109280. https://doi.org/10.1016/j.engstruct.2019.109280
19. Vecchio FJ, Collins MP. Modified compression-field theory for reinforced concrete elements subjected to shear. J Am Concr Inst. 1986;83:219–31. https://doi.org/10.14359/10416
20. Bentz EC. Sectional analysis of reinforced concrete members. Ottawa, Canada: University of Toronto; 2000b.
21. Paasikallio K. Stress and strain analysis of cracked reinforced concrete panels. Finland: Helsinki University of Technology; 1992.
22. Bentz EC. Membrane 2000. 2000.
23. Kujala J. Prestressed concrete girders made continuous - continuity tests. Tampere, Finland: Tampere University; 2020.
24. Jonasson J-E. Studier rörande T-balkar med dragen fläns (studies of T-beams with the flange in tension). Stockholm, Sweden: Royal Institute of Technology; 1976.
25. CEB-FIP. FIB Bulletin 2, structural concrete, basis of design; 1999
26. Amadio C, Fedrigo C, Fragiacomo M, Macorini L. Experimental evaluation of effective width in steel-concrete composite beams. J Constr Steel Res. 2004;60(2):199–220. https://doi.org/10.1016/j.jcsr.2003.08.007
27. EN 1993-1-5. Eurocode 3: design of steel structures - Part 1–5: plated structural elements; 2006
28. Luo D, Zhang Z, Li B. Shear lag effect in steel-concrete composite beam in hogging moment. Steel Compos Struct. 2019;31(1):27–41. https://doi.org/10.12989/scs.2019.31.1.027

AUTHOR BIOGRAPHIES

Ulla Kytölä, Ph. D. student
Unit of Concrete and Bridge Structures
Tampere University
Tampere, Finland
ulla.kytola@tuni.fi

Joonas Tulonen, Ph. D. student
Unit of Concrete and Bridge Structures
Tampere University
Tampere, Finland
joonas.tulonen@tuni.fi

Anssi Laaksonen, Professor
Unit of Concrete and Bridge Structures
Tampere University
Tampere, Finland
anssi.laaksonen@tuni.fi

How to cite this article: Kytölä U, Tulonen J, Laaksonen A. Longitudinal shear in the tension flanges of composite concrete beams made continuous. Structural Concrete. 2021;1–18. https://doi.org/10.1002/suco.202100561